Korea Polymer Journal, Vol. 9, No. 4, pp 210-219 (2001)

Structural Changes of Biodegradable Poly(tetramethylene succinate) on Hydrolysis

Jick Soo Shin, Eui Sang Yoo, and Seung Soon Im

Department of Textile Engineering, Hanyang University, Seoul, Korea

Hyun Hoon Song*

Department of Polymer Science and Engineering, Hannam University, Daejon , Korea

Received April 4, 2001

Abstract : Quenched and slow cooled as well as isothermally crystallized poly(tetramethylene succinate) (PTMS) films at two different temperatures were prepared. In the process of hydrolysis of the four specimens, structural changes such as the crystallinity, crystal size distribution, lattice parameter, lamellar thickness, long period and surface morphology were investigated by using wide and small angle X-ray scattering (WAXS and SAXS), differential scanning calorimetry (DSC) and scanning electron microscopy (SEM). The hydrolytic degradation of quenched film was faster than that of slow cooled and isothermally crystallized films. The film crystallized at 100°C exhibited extensive micro voids and thus showed faster degradation than that crystallized at 75°C, demonstrating surface morphology is another important factor to govern degradation rate. The crystallinity of the specimen increased by 5~10% and long period decreased after hydrolysis for 20 days. At the initial stage of degradation, the lamellar thickness of quenched film rather increased, while that of slow cooled and isothermally crystallized films decreased. The hydrolytic degradation preferentially occurred in the amorphous region. The hydrolytic degradation in crystal lamellae are mainly at the crystal surfaces.

Introduction

Durability and anti-microbial stability of plastics which have been thought to be favorable characteristics of synthetic polymers became ecological and environmental problems because they do not degrade after disposal. Biodegradable polymers have been considered as a possible solution for the ecological and environmental problem of the huge amount of plastic waste.[1-11] Aliphatic polyesters presently constitute the most attractive class of artificial polymers which can degrade in contact with living tissues or under outdoor conditions. Work has been in progress for the last two decades which has led to their applications in surgery and in pharmacology. These compounds are also of interest for outdoor applications such as packaging materials or mulch films and implant therapy by controlled delivery of pesticides or insecticides in agriculture, although they are still too expensive. Factors which can affect their biodegradation have been investigated world-wide. However, the literature contains confusing statements and controversial data.

Polymer morphology plays a critical role in degradation phenomena. It is now well known that degradation of semicrystalline polymers occurs in two stages. The first stage consists of water-diffusion into the amorphous regions with random hydrolytic scission of ester bonds. The second stage starts when most of the amorphous regions are degraded. Hydrolytic attack then progresses within crystalline domains.[12-14] Fredericks *et al.* studied structure and morphology changes of Vicryl sutures *in vitro*.[14] They reported that hydrolytic attack was initiated in the amorphous area of the polymer, resulting in an augmentation of crystallinity. As

*e-mail : songhh@mail.hannam.ac.kr

hydrolysis advanced, crystalline areas were attacked and eventually removed.

The increase in crystallinity during hydrolytic degradation was observed in both poly(glycolic acid) (PGA) and PGA-co-PLA samples.[14-18] This has been explained by cleavage-induced crystallization as the tie chains in the amorphous regions can degrade into fragments, resulting in a lesser degree of entanglement by the long-chain molecules in the amorphous regions.

Ginde and Gupta examined the influence of polymer morphology on the chemical degradation of PGA fibers and pellets.[19] The degradation rate was found much faster for pellets than for fibers and regarded as in agreement with the presence of long-range order in fibers. The commercial pellets had higher degree of crystallinity (38%) than with melt-spun fibers (35%). However, X-ray diffraction results showed the former was lack of orientation. Thus, chain orientation also plays an important role in the hydrolytic degradation.[19] Y. Tokiwa *et al.* revealed that the biodegradability of aliphatic polyesters depends upon melting points which is determined by the chemical structure.[20] Other workers reported the physical or chemical characters of polymers and biodegradability.[21-23]

In the case of poly(tetramethylene succinate) (PTMS), however, little literature is available on morphological understanding of degradation process. In this paper, we attempted to identify the effects of various morphological parameters on the hydrolytic degradation of PTMS. In particular, efforts were focused on the microstructural changes such as crystallinity, crystal size or crystal perfectness, lattice parameter, lamellar thickness and long period during degradation process.

Exprimental

Materials and Sample Preparation. PTMS (SG1109) obtained from SKI, Ltd. of Korea was used after drying for over 48 hrs in vacuum at room temperature. Specimens were prepared in the form of thin films (surface area 9 cm^2) using a hot press at 150 °C. To control the polymer morphology the specimens were crystallized under four different crystallization conditions: rapid quenching ($\phi_{mc}=42\%$), slow cooling (3 °C/min) ($\phi_{mc}=53\%$) and isothermal crystallization at 75 °C ($\phi_{mc}=55\%$) and 100 °C ($\phi_{mc}=57\%$) for 2 hrs and 12 hrs, respectively, in a curing bath.

Hydrolysis. Hydrolysis was performed in 100 ml buffer solutions at pH 12 and the solutions were stirred at 100 rpm in a stirring bath maintained at 40 °C. Degraded films were collected per desired time and dried for 24 hrs in a vacuum desiccator at room temperature before measuring the weight loss and examining the morphology changes. Degradability was obtained by the following equation (1):

$$\text{Degradability}(\%) = \frac{A-R_s}{A} \quad (1)$$

where A is the amount of initial polymer specimen (mg), R_s is the amount of specimen remaining after the degradation (mg).

Structure Characterization. The melting behavior of PTMS films was studied by using a DSC (Perkin-Elmer DSC 7) at a heating rate of 10 °C/min under nitrogen atmosphere. The apparatus was precalibrated with an indium standard.

To examine the microstructural changes upon hydrolytic degradation, wide and small angle X-ray scattering (WAXS and SAXS) were performed. For the WAXS experiment, a powder diffractometer attached to a Rigaku rotating anode generator (CuKα radiation, λ = 1.542 Å, 40 kV, 160 mA) was used. Scattered intensities were collected at the scattering angles of 10-40°. For the SAXS measurement, a Kratky camera with a slit-type beam geometry was used. SAXS intensities were collected at the scan speed of 0.05°/min and 2θ from 0.1° to 3°. After SAXS intensity profile was corrected for the background scattering and Lorentz factor, relative scattered intensity was obtained as a function of scattering vector q (= $4\pi \sin(\theta)/\lambda$).

In addition to the internal structure, surface morphology of the film was also examined by a scanning electron microscopy (SEM) (TOPCON, SX-30) before and after the hydrolysis.

Results and Discussion

Degradation of PTMS. In Figure 1, the weight

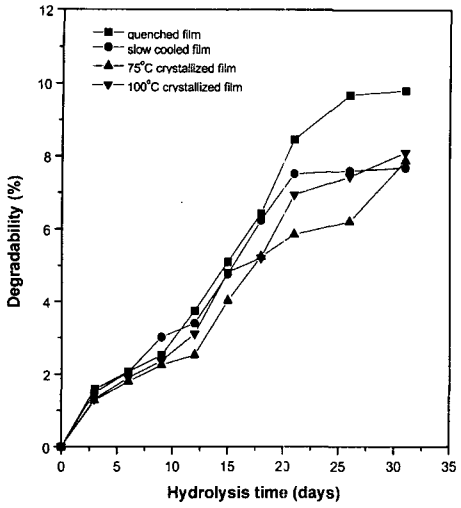

Figure 1. Variation of degradability of PTMS films.

losses of PTMS films prepared under different crystallization conditions are compared upon hydrolysis in a buffer solution of pH 12 up to 32 days. PTMS films could not maintain their apparent shape after hydrolysis for 32 days, indicating extensive chain scissions in amorphous region. The curves in the figure exhibit that the degradation of quenched film was faster than slow cooled and isothermally crystallized films. This result can be related to a low degree of crystallinity and poor chain packing as well as small crystal size in quenched film. In our previous report,[24] isothermally crystallized PTMS films at over 70 °C showed well defined spherulites with crystallinity higher than 50%. On the other hand, quenched film exhibited relatively small crystallites and about 40% crystallinity. The degradability of quenched sample reached up to 10% after 26 days of hydrolysis and then was level-off.

In general, degradation rate and degradability decrease with increasing crystallinity. However, the film crystallized at 100 °C with 57% crystallinity shows almost same degradability as the slow cooled film and exhibits even faster degradation rate than that crystallized at 75 °C during 26 days of hydrolysis. We found this unusual results is associated with the micro voids formation in the samples, especially on the surface. In the last section, micro voids observed in films will be discussed on the basis of SEM results.

Thermal Analysis. Curves in Figure 2 represent the DSC heating scans of PTMS films after hydrolysis in a buffer solution of pH 12. As discussed previously the degradability measurement was stopped after 32 days of hydrolysis due to the extensive corruption of the samples. However, we were able to continue DSC and X-ray scattering experiment up to 82 days of hydrolysis.

In Figure 2(a), DSC heating curves of rapidly quenched film are shown. The curves reveal a broad exothermic peak (50~90 °C), indicating cystallization during heating. It is interesting to note that the exothermic peak becomes more obvious as hydrolysis time increases. The increase of exotherms with hydrolysis might be associated with an increase of chain mobility due to chain scissions mainly in the amorphous region. The melting temperature slightly increases for the first 18 days of hydrolysis and remains in constant until 61 days but notably decreases after 82 days of hydrolysis. The decrease of melting temperature of quenched sample during hydrolysis could be explained on the basis of the origin of melt endotherm as discussed below.

Unlike the quenched sample, slow cooled and isothermally crystallized film show distinct double melting endotherms(Figure 2(b) and 2(c)). In the previous report[25] on melting behavior of PTMS, low temperature melting endotherm was attributed to the melting of original crystals and the high temperature endotherm was to the melting of new crystals formed in melt-recrystallization process. And the broad melting endotherm observed in the quenched films could be regarded as a superimposed peak of a few melting endotherms from melt-recrystallization phenomenon (note that the high endothermic peak positions in Figure 2(b) and 2(c) are nearly identical to the peak in Figure 2(a)). Consequently, because the maxima of melting endotherm of quenched sample is correspondent to the melting of recrystallized crystals during heating, the maxima should move to a lower temperature when the degradation occurred in molecular chains, thus resulting in small and less perfect recrystallized crystals during DSC scan.

In Figure 2(b) and 2(c), the maxima of low endotherm shifts to the higher temperature at 9 days of hydrolysis, which is probably due to the

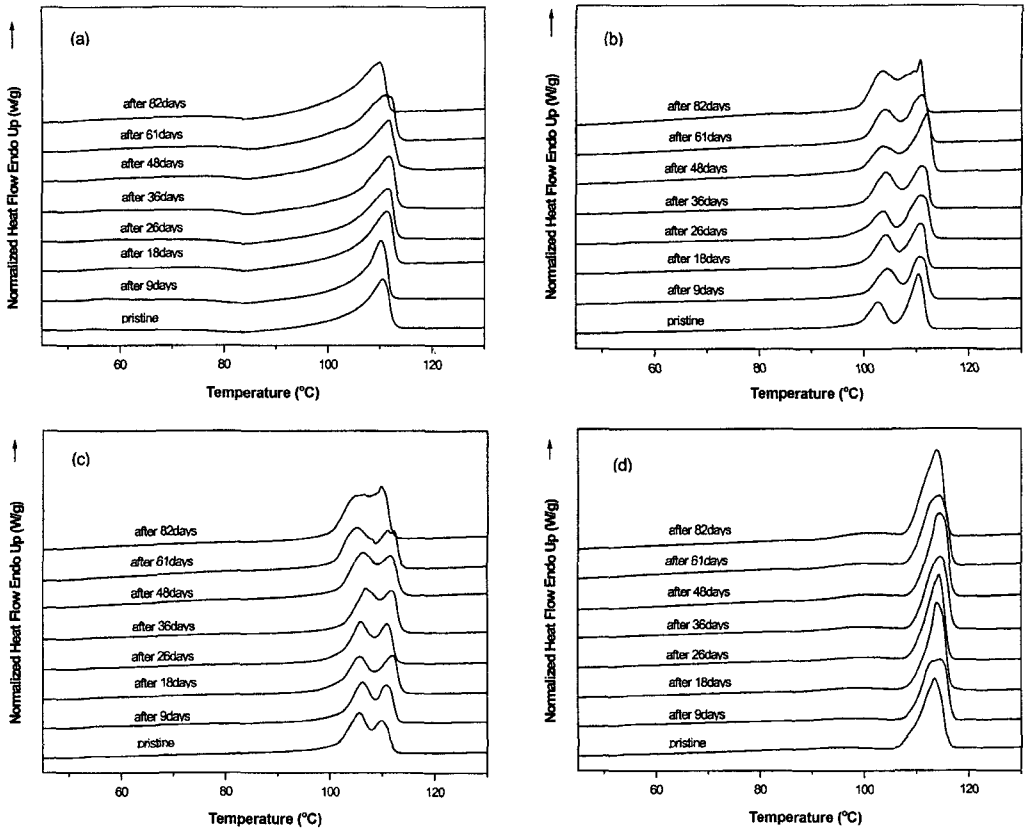

Figure 2. Variation of DSC results for (a) quenched, (b) slow cooled, (c) 75 °C crystallized, and (d) 100 °C crystallized PTMS films with hydrolysis.

cleavage-induced crystallization resulted from the increase of chain mobility by chain scissions in amorphous region. After hydrolysis for 9 days, however, low endotherm moves to the lower temperature, indicating the onset of the degradation of crystalline region. The high endotherm in Figure 2(b) and 2(c) show nearly identical behavior to that of quenched film (Figure 2(a)), supporting the identical origin as discussed previously.

Films crystallized at 100 °C (Figure 2(d)) reveals only a single melting endotherm, which has been well explained in the previous report.[25] It is also noted that the peak position slightly decreases with hydrolysis time.

Microstructural Changes During Hydrolysis. In Figure 3, WAXS patterns obtained from the films after predetermined hydrolysis time are plotted. Figure 3(a) represents the quenched films, Figure 3(b) for the slow cooled ones, Figure 3(c) and 3(d) for the isothermally crystallized PTMS films at 70 and 100 °C, respectively. Three strong reflection peaks, located at 19.7, 22.0 and 22.8° are indexed as (020), (021) and (110) respectively based on the monoclinic unit cell.[26] The diffraction peaks are stronger and sharper with the ones of slower cooling rate and higher cystallization temperature, indicating the better crystalline order.

Another prominent result observed in the diffraction patterns is that the diffraction peaks of (110) and (021) plane are broadened with the treatment time. The broadening of the diffraction peaks can be related to either the reduction in crystal size or the reduction in crystal packing order. Change of half width upon hydrolysis for (110) and (021) plane are presented in Figure 4 (a) and 4(b), respectively. The half width of (110) plane provides the average crystal dimension in a

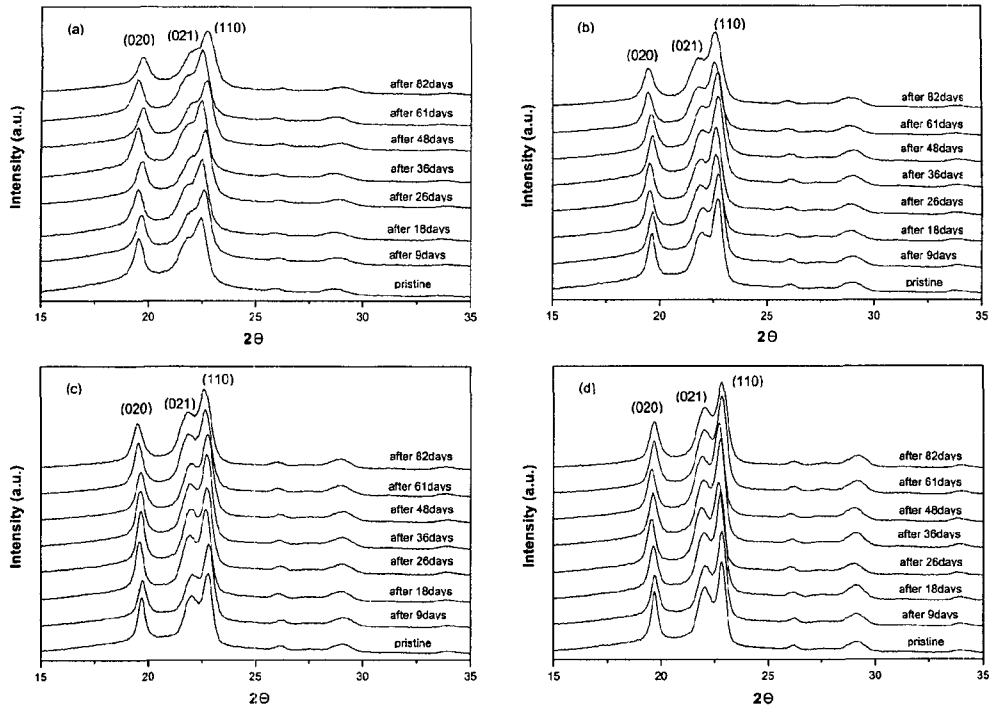

Figure 3. WAXS patterns for (a) quenched, (b) slow cooled, (c) 75 °C crystallized, and (d) 100 °C crystallized PTMS films with hydrolysis.

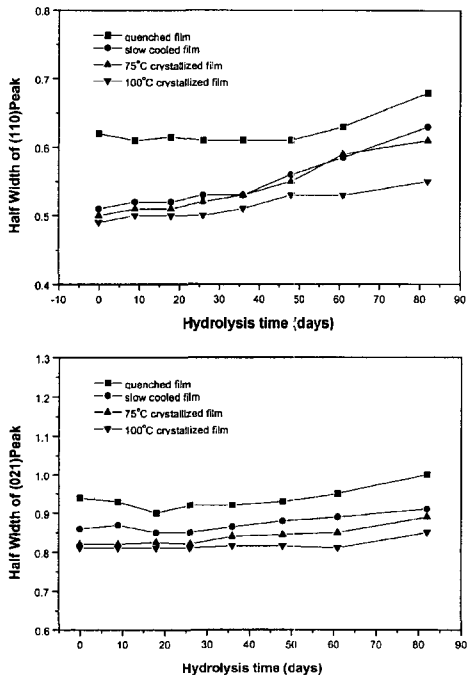

Figure 4. The half width of (100) and (021) peak with hydrolysis.

and b crystal axis, i.e, the lateral size of lamella, while the half width of (021) provides the information related to the lamellar thickness. The half widths of (110) for slow cooled and isothermally crystallized films increase monotonously with hydrolysis, while quenched film shows no changes in this term until 50 days, which is probably due to the effect of cleavage-induced crystallization. The increment of the half width of (110) plane implies that the degradation takes place at the side direction of lamellar, while (021) plane is at the lamellar surface. The half width of (021) plane associated with crystal size in c-axis, therefore the lamellar thickness, shows no change until 26 days of hydrolysis in slow cooled and isothermally crystallized. After hydrolysis for 26 days, the half width of (021) plane slightly increases (Figure 4(b)). Comparing the results of (110) and (021) plane, it is apparent that the degradation, in slow cooled and isothermally crystallized films, occurs mainly at the side of lamellar units during the early stage of degradation. On the other hand, in the beginning of hydrolysis of quenched films, the

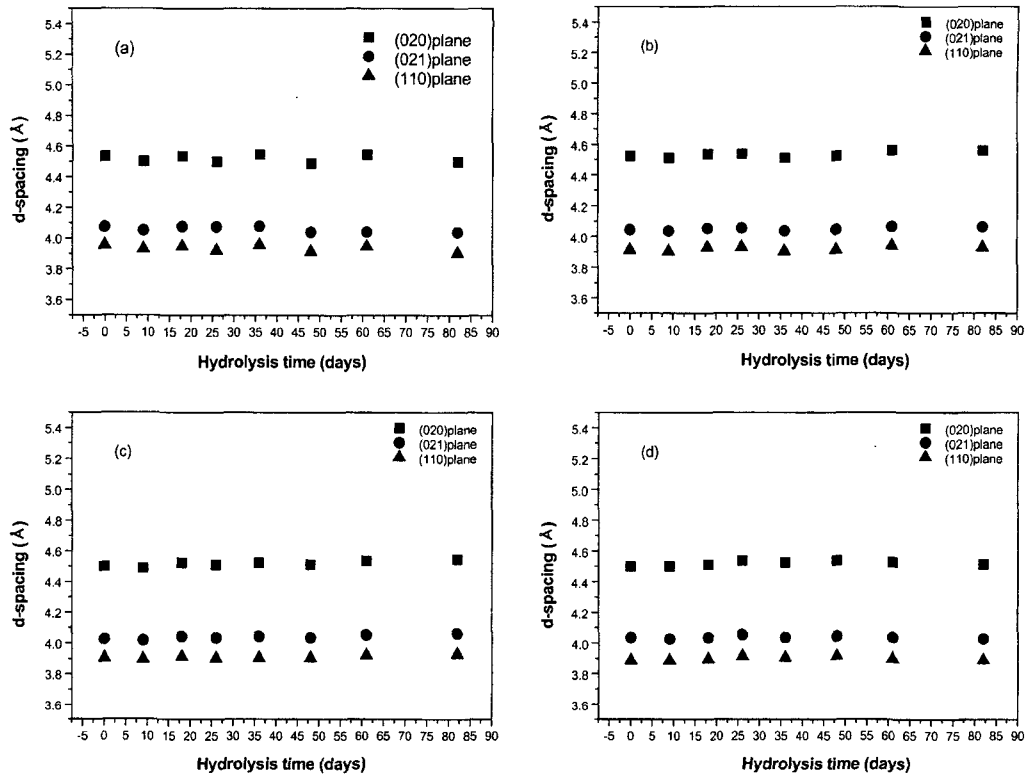

Figure 5. Change in d-spacing of (a) quenched, (b) slow cooled, (c) 75 °C crystallized, and (d) 100 °C crystallized PTMS films with hydrolysis.

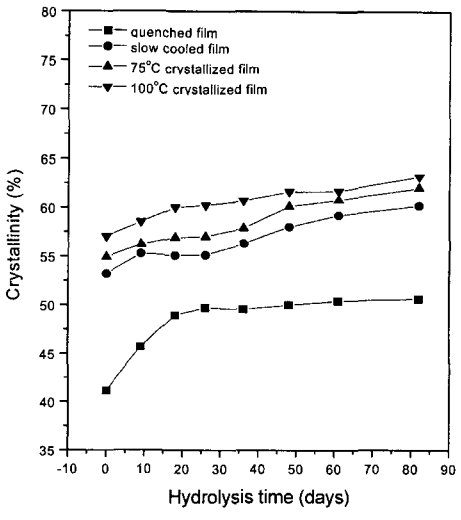

Figure 6. Variation of crystallinity with hydrolysis.

half width of (010) and (021) plane decreases, which can be attributed to the cleavage-induced crystallization and annealing effects at the hydrolysis temperature of 40 °C.

In Figure 5, changes of d-spacing evaluated from the positions of (110), (020), and (121) reflections are plotted. There is no significant change in lattice parameters in all four samples during the prolonged hydrolysis process. It is apparent that the water can not penetrate into the crystal lattice, suggesting hydrolysis only takes place at the surfaces of the crystallites.

From the WAXS profiles the mass degree of crystallinity (ϕ_{mc}) was obtained and is plotted in Figure 6. It is apparent that the crystallinity of films increased with the increase of treatment time. All three samples, except quenched one, show a gradual and monotonic increase in the crystallinity with increasing hydrolysis time, while the quenched film shows a rapid 8% increment in crystallinity within 26 days of hydrolysis and then levels off. Such increment of the crystallinity in the process of degradation can be easily attributed to the reduction of amorphous region by hydrolysis.

However, we also note that the increase of crystallinity in quenched film is achieved for initial 26 days. We recall that the degradability calculated from the weight loss after hydrolysis for 26 days is under 10% (Figure 1). Supposing that the degradation occurs mainly in the amorphous portion, 10% degradability corresponds to about 5% increase in crystallinity. The difference between these two values of the crystallinity implies that other effects, in addition to the removal of amorphous region, may cause an increase in the crystallinity. This effect was already explained by the cleavage-induced crystallization as the tie chains in the amorphouss regions degrade into fragments. In the case of slow cooled and isothermally crystallized films at 75 and 100 °C, about 5% increase of crystallinity is noted after 26 days of hydrolysis. The value agrees well with the increment of degradation as shown in Figure 1.

Figure 7 represents the selected SAXS profiles obtained from PTMS films during hydrolysis. In these figures, it is apparent that the peak maxima, originating from the lamellar stacks where the amorphous layers are located in between, shifts to a high q and the scattering intensity increases with the hydrolysis. The increase of SAXS intensity can be attributed to the increase of electron density contrast between the lamella and the amorphous layer. And the increase of density contrast is originating from the preferred degradation in amorphous region.

In Figure 8, long period (L) evaluated by the Bragg equation from the SAXS profiles is plotted. It is shown that the value of L from the quenched films is the lowest among those of three samples. In the case of slow cooled and isothermally crystallized films, the value of L decreases rapidly during hydrolysis but much slower rate is noted in the quenched film. This is again related to the lamellar thickening associated with cleavage-induced crystallization during the early stage of hydrolysis. Careful examination of the curve (quenched film in Figure 7) reveals a plateau for the first 20 days of hydrolysis, supporting the crystallization. Figure 9 exhibits values of lamellar thickness (l_c) against the hydrolysis time, being calculated from the long period and the crystallinity. In the case of quenched film, value of lamellar thickness (l_c) is

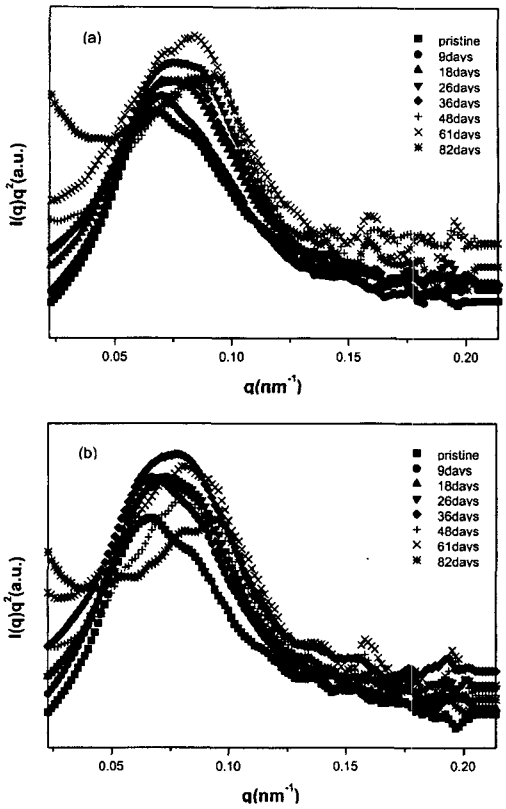

Figure 7. Lorents corrected SAXS patterns after hydrolysis; (a) slow cooled and (b) 75 °C crystallized PTMS films.

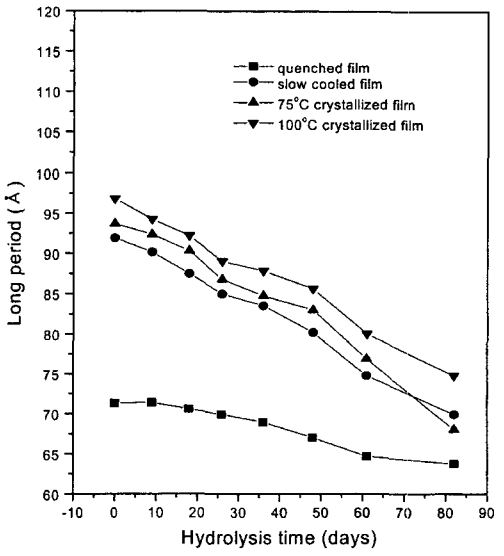

Figure 8. Variation of long periods with hydrolysis.

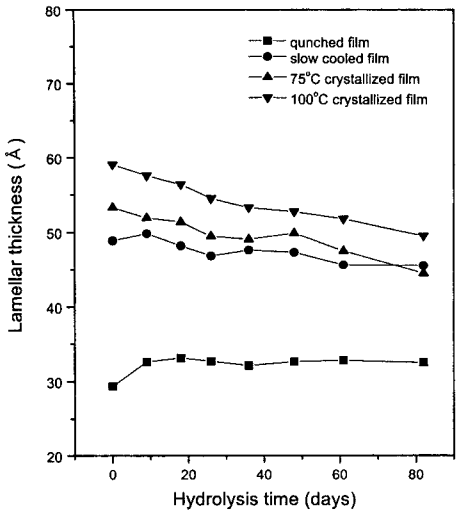

Figure 9. Variation of lamellar thickness with hydrolysis.

found to increase untill 26 days of hydrolysis and then remains nearly constant during the subsequent period. Again the lamellar thickening can be observed at the initial stage which is associated with the crystallization due to annealing effect and an increase of mobility, as was suggested by the results of the half width, crystallinity and long period. Only a minimal and gradual decrease of lamellar thickness is noted in slow cooled and isothermally crystallized films, indicating a minimal surface degradation. The morphological parameters during hydrolysis of PTMS films are summarized in Table I.

In Figure 10, SEM micrographs of PTMS film surface before hydrolysis are compared. In the figure, we note that the film crystallized at 100°C contains higher population of micro voids on the surface (10~30 μm) than other films. When the material is crystallized, internal stresses are building up, resulting in lamellae collapse in a cooperative manner and thus creating large voids. The size and number of existing voids increase with hydrolytic degradation. It supports the hypothesis that micro voids are involved in the rapid release of degradation products. The difference of surface morphology caused by crystallization temperature (ca. 100°C) accounts for the different degradation behavior seen in Figure 1. After hydrolysis for 32 days, the structure of the matrix becomes completely different. The surface of hydrolized PTMS films shows the presence of cavities in the form of ridges and valleys (Figure 11). Our observation was consistent with this fact; that is, the initial stage of hydrolytic degradation may be a random scission of the ester linkage of chain in the amorphous region, resulting in selective erosion of the amorphous regions, which is probably necessary for further hydrolytic attack on the crystalline regions. Then the exposed spherulites were subse-

Table I. Morphological Parameters for PTMS Films during Hydrolysis

		Time (days)							
		0	9	18	26	36	48	61	82
Quenched Film	L(Å)	71.2	71.3	70.6	69.9	68.9	67	64.6	63.7
	l_c(Å)	29.3	32.6	33.1	32.6	32	32.6	32.7	32.4
	ϕ_{mc}(%)	41.6	45.6	48.9	49.7	49.5	50	50.4	50.6
Slow Cooled Film	L(Å)	91.9	90.1	87.4	84.9	83.5	80.1	74.7	69.9
	l_c(Å)	48.8	49.8	48.1	46.8	47.6	47.3	45.6	45.5
	ϕ_{mc}(%)	53.1	55.26	55.09	55.1	56.3	58	59.2	60.2
75°C Crystallized Film	L(Å)	93.6	92.3	90.3	86.7	84.7	82.9	76.8	68
	l_c(Å)	53.3	51.9	51.3	49.4	49	49.8	47.4	44.4
	ϕ_{mc}(%)	54.9	56.2	56.8	57	57.8	60.1	60.7	62
100°C Crystallized Film	L(Å)	96.8	94.2	92.1	89	87.8	85.6	80	74.7
	l_c(Å)	59	57.5	56.4	54.5	53.3	52.7	51.7	49.4
	ϕ_{mc}(%)	57	58.5	60	60.2	60.6	61.6	61.6	63.1

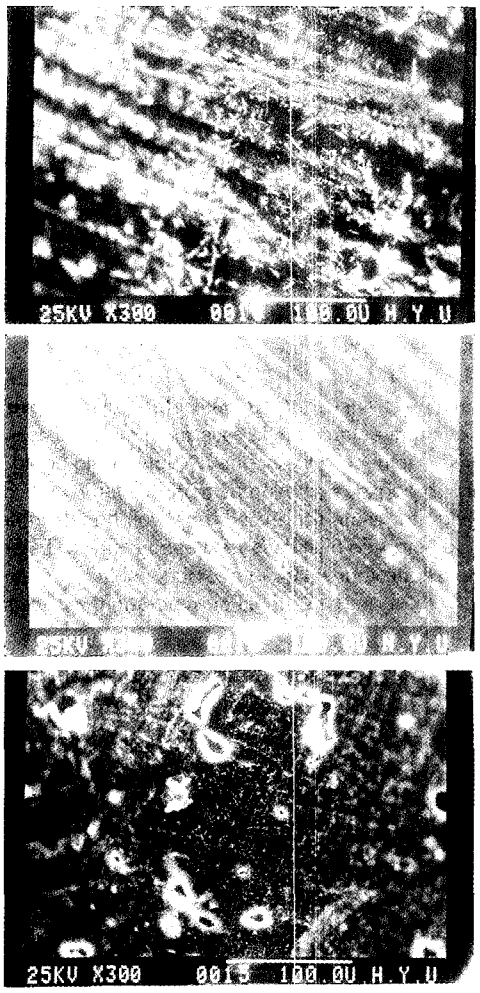

Figure 10. Scanning electron micrographs of pristine PTMS films; (a) quenched, (b) 75 °C crystallized, and (c) 100 °C crystallized.

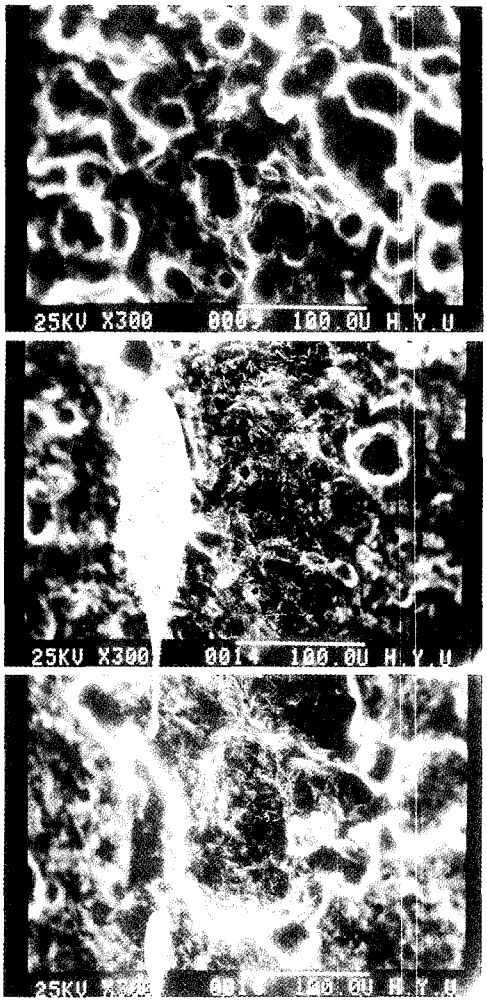

Figure 11. Scanning electron micrographs of hydrolyzed PTMS films; (a) quenched, (b) 75 °C crystallized, and (c) 100 °C crystallized.

quently degraded.

Conclusions

The higher degradation rate in quenched film was attributed to a lower degree of crystallinity and lower packing order of molecular chains. Isothermally crystallized films at 100 °C showed higher degradability than isothermally crystallized films at 75 °C, which was attributed to micro voids formation. The crystallinity increased significantly in all the samples during the initial degradation period. This behavior can be explained by two reasons; the reduction of amorphous region and the cleavage-induced crystallization. There was a relatively less change of long period (L) in the quenched film, while a notable change was observed for the slow cooled and isothermally crystallized films. The lamellar thickness (l_c) of quenched films increased during 26 days of hydrolysis, while that of slow cooled and isothermally crystallized films decreased after hydrolysis for 20 days. During the initial stage of degradation of quenched film, the crystallization, caused by annealing effects and an increase of mobility due to chain scissions in amorphous region, takes

place simultaneously. Within our hydrolysis condition and time scale, the degradation mainly occurred in the amorphous regions. The hydrolytic degradation in crystalline regions took place only at the crystal surfaces.

Acknowledgment. This work was financially supported by KOSEF (#971-1102-013-2).

References

(1) R. Narayan, in *Science and Engineering of Composing: Design, Environmental Microbiological and Utilization Aspects,* H. A. J. Hoitink and H. M. Keener, Eds., Renaisance Publication, Ohio, 1993.
(2) G. S, Kumor, V. Kalpagam, and U. S. Nandi, *ibid.*, **C22** (2), 225 (1982-1983).
(3) J. S. Singhal, H. Singh, and A. R. Ray, *J. Macromol. Sci. Rev. in Macromol. Chem.*, **C28** (384), 475 (1988).
(4) M. Vert and D. Angew. *Macromol. Chem.*, **166**, 55 (1998).
(5) S. J. Huang, *Encyclopedia of Polymer Science and Engineering,* 2nd edn, John Wiley & Sons, New York, 1985, pp. 220.
(6) S. J. Juang, in *Comprehensive Polymer Science,* Pergamon Press, London, 1989, pp. 567.
(7) D. L. Kaplan, J. M. Mayer, and D. Ball, *et al.*, in *Biodegradable Polymer and Packaging*, Techonmics Publishing, Lancaster-Basel, 1993, pp. 1.
(8) G. Swift, *Acc. Chem. Res.*, **26**, 105 (1993).
(9) R. Lens, in *Advances in Polymer Series,* Springer-Vierlanger, 1993, pp. 1.
(10) A. C. Albertsson and S. Karlsson, in *Comprehensive Polymer Science, First Supplement,* Pergamon Press, London, pp. 285.
(11) J.-C. Huang, A. S. Shetty, and M. -S. Wang, *Adv. Polym. Technol.*, **10**, 23 (1990).
(12) E. W. Fischer, H. J. Sterzel, and G. Wegner, *Kolloid-Z. u. Z. Polymere,* **251**, 980 (1973).
(13) B. K. Carter, G. L. Wilkes, S. W. Shakaby, A. S. Hoffman, B. D. Ratner, and T. A. Horbett, Eds., *Polymers as Biomaterials,* Plenum Press, New York, 1984, pp. 67.
(14) R. J. Fredericks, A. J. Melveger, and L. J. Dolegiewtz, *J. Polym. Sci.; Polym. Phys. Ed.*, **22**, 57 (1984).
(15) C. C. Chu, *J. Appl. Polym. Sci.*, **26**, 1727 (1981).
(16) C. C. Chu and N. O. Combell, *J. Biomed. Mater. Res.*, **16**, 417 (1982).
(17) A. Browing and C. C. Chu, *J. Biomed. Mater. Res.*, **20**, 613 (1986).
(18) E. King and R. E. Cameron, *J. Appl. Polym. Sci.*, **66**, 1681 (1997).
(19) R. M. Ginde and R. K. Gupta, *J. Appl. Polym. Sci.*, **33**, 2411 (1987).
(20) T. Tokiwa, T. Ando, T. Suzuki, and T. Takeda, *Agric. Biol. Chem.*, **21**, 988 (1980).
(21) T. Nakamura, S. Hitomi, and S. Watanabe, *et al.*, *J. Biomed. Mater. Res.*, **23**, 1115 (1986).
(22) R. A. Miller, J. M. Brady, and D. E. Cutright, *J. Biomed. Mater. Res.*, **11**, 711 (1977).
(23) J. W. Leeslag, S. Gogolewski, and A. J. Pennings, *J. Biomed. Mater. Res.*, **29**, 2829 (1984).
(24) E. S. Yoo and S. S. Im, *Bulletin of the Korea Chemical Society,* **18**, 350 (1997).
(25) E. S. Yoo and S. S. Im, *J. Polym. Sci. Part B: Polymer Physics,* **37**, 1375 (1999).
(26) K. J. Ihn, E. S. Yoo, and S. S. Im, *Macromolecules,* **28**, 2460 (1995).